Hybrid Singular Element Design for the Bending Analysis of Bimaterial Thin Cracked Plates

Wen-Hwa Chen* and Chyan-Bin Hwu†
National Tsing Hua University
Hsinchu, Taiwan, China

Introduction

THE problems of bending of homogeneous thin cracked plates have been investigated by several researchers[1-6] using different finite element approaches. For bimaterial thin cracked plates, however, there has been very little work done.[7]

This Note hopes to extend the work in Ref. 6 and to devise a new hybrid singular crack element to deal with thin bimaterial plates containing an interface crack and subjected to bending loadings. To account for the singular and oscillatory characters of the stress field near the crack tip, the assumed interpolation functions are basically derived from the displacement and stress fields given by Sih and Rice.[7] The proposed stress intensity factors are defined and evaluated. The influences of material properties on the transverse deflection and stress intensity factors are then evaluated. The results presented should be of help in further studies of bimaterial crack problems.

Hybrid Singular Element Design

As shown in Fig. 1, a 21 degree-of-freedom rectangular hybrid singular bending crack element is designed in this work for the analysis of bimaterial cracked problems. To devise such an element, the three similar independent variables as noted in Ref. 6 can be assumed to be

$$w = \lfloor U_R \rfloor \{\beta\} + \lfloor U_S \rfloor \{K_H\} \tag{1}$$

$$\begin{Bmatrix} w^* \\ \theta_n^* \end{Bmatrix} = [L]\{q\} \tag{2}$$

$$\begin{Bmatrix} V_n \\ -M_{nn} \end{Bmatrix} = [R]\{\alpha\} \tag{3}$$

where the column matrices $\{\alpha\}$ and $\{\beta\}$ are independent parameters that can be determined through the stationary condition of the modified principle of minimum total potential energy and $\{K_H\}$ and $\{q\}$ are the column matrices of the proposed stress intensity factors and appropriate nodal values. The interpolation functions $\lfloor U_R \rfloor$ and $\lfloor U_S \rfloor$ used for the element interior lateral displacement w in Eq. (1) are assumed to be regular polynomials and proper asymptotically correct displacement functions near the crack tip,[7] respectively. The interelement boundary displacement w^* and normal slope θ_n^* in Eq. (2) can be determined uniquely in terms of the relevant $\{q\}$ through the interpolation function $[L]$. The interpolation function $[R]$ on the element boundary in Eq. (3), for the equivalent boundary transverse shear V_n and bending moment M_{nn}, is derived from the assumed singular stress field near the crack tip.

Element Interior Lateral Displacement Field w

The interpolation function $\lfloor U_R \rfloor$ as shown in Eq. (1) can be taken as the same one as in Ref. 6. However, for the interpolation function $\lfloor U_s \rfloor$, it can be assumed as

$$\lfloor U_s \rfloor_1 = \frac{1-\bar{\nu}^2}{\sqrt{2}\bar{E}\bar{h}(3+\bar{\nu})} \left\lfloor \frac{[(3/2)-2k^2]e^{-k\pi}}{16k^2+[(3/2)-2k^2]^2} U_{s1}^1 - \frac{4ke^{-k\pi}}{16k^2+[(3/2)-2k^2]^2} U_{s1}^2 \quad \frac{4ke^{-k\pi}}{16k^2+[(3/2)-2k^2]^2} U_{s1}^1 + \frac{[(3/2)-2k^2]e^{-k\pi}}{16K^2+[(3/2)-2k^2]^2} U_{s1}^2 \right\rfloor$$

and

$$\lfloor U_s \rfloor_2 = \frac{1-\bar{\nu}^2}{\sqrt{2}\bar{E}\bar{h}(3+\bar{\nu})} \left\lfloor \frac{[(3/2)-2k^2]e^{-k\pi}}{16k^2+[(3/2)-2k^2]^2} U_{s2}^1 - \frac{4ke^{-k\pi}}{16k^2+[(3/2)-2k^2]^2} U_{s2}^2 \quad \frac{4ke^{-k\pi}}{16k^2+[(3/2)-2k^2]^2} U_{s2}^1 + \frac{[(3/2)-2k^2]e^{-k\pi}}{16K^2+[(3/2)-2k^2]^2} U_{s2}^2 \right\rfloor$$

where $\lfloor U_s \rfloor_1$ and $\lfloor U_s \rfloor_2$ represent the interpolation functions of material 1 and 2, respectively. In the above,

$$U_{s1}^1 = 2e^{k\theta} r^{3/2} \left[\cos\left(\frac{\theta}{2} + k\log r\right) - \frac{3+\nu_1}{1-\nu_1} e^{2k(\pi-\theta)} \cos\left(\frac{3\theta}{2} + k\log r\right) + \sin\theta \sin\left(\frac{\theta}{2} - k\log r\right) - 2k\sin\theta\cos\left(\frac{\theta}{2} - k\log r\right) \right]$$

$$U_{s1}^2 = 2e^{k\theta} r^{3/2} \left[-\sin\left(\frac{\theta}{2} + k\log r\right) + \frac{3+\nu_1}{1-\nu_1} e^{2k(\pi-\theta)} \sin\left(\frac{3\theta}{2} + k\log r\right) - \sin\theta\cos\left(\frac{\theta}{2} - k\log r\right) - 2k\sin\theta\sin\left(\frac{\theta}{2} - k\log r\right) \right]$$

$$U_{s2}^1 = 2\gamma \frac{\mu_1}{\mu_2} e^{k(\theta+2\pi)} r^{3/2} \left[\cos\left(\frac{\theta}{2} + k\log r\right) - \frac{3+\nu_2}{1-\nu_2} e^{-2k(\pi+\theta)} \cos\left(\frac{3\theta}{2} + k\log r\right) + \sin\theta \sin\left(\frac{\theta}{2} - k\log r\right) - 2k\sin\theta\cos\left(\frac{\theta}{2} - k\log r\right) \right]$$

$$U_{s2}^2 = 2\gamma \frac{\mu_1}{\mu_2} e^{k(\theta+2\pi)} r^{3/2} \left[\sin\left(\frac{\theta}{2} + k\log r\right) - \frac{3+\nu_2}{1-\nu_2} e^{-2k(\pi+\theta)} \sin\left(\frac{3\theta}{2} + k\log r\right) + \sin\theta\cos\left(\frac{\theta}{2} - k\log r\right) + 2k\sin\theta\sin\left(\frac{\theta}{2} - k\log r\right) \right]$$

where

$$k = -\frac{1}{2\pi} \log\left[\frac{\mu_1}{\mu_2}\left(\frac{\mu_2+\gamma}{\gamma\mu_1+1}\right)\right]$$

$$\mu_i = \frac{3+\nu_i}{1-\nu_i}, \quad i = 1,2$$

$$\gamma = \frac{D_1}{D_2}\left[\frac{1-\nu_1}{1-\nu_2}\right] \qquad D_i = \frac{E_i h_i^3}{12(1-\nu_i^2)}$$

Received Oct. 15, 1985; revision received Dec. 16, 1985.

*Professor and Head, Department of Power Mechanical Engineering.
†Graduate Student, Department of Power Mechanical Engineering.

E_i, ν_i, h_i, and D_i denote Young's modulus, Poisson's ratio, thickness, and the flexural rigidity of plate i, respectively. k is defined as the bielastic constant. For homogeneous cases, $k=0$. $\bar{E}$, $\bar{\nu}$, and $\bar{h}$ are the mean values of corresponding parameters of plate 1 and 2,

$$\{K_H\}^T = \lfloor \tilde{K}_1, \tilde{K}_2 \rfloor$$

where the proposed stress intensity factors k_1 and k_2 can be defined as

$$\tilde{K}_1 = e_i \frac{\bar{E}\bar{h}(3+\bar{\nu})(1-\nu_i^2)}{E_i h_i (3+\nu_i)(1-\bar{\nu}^2)} \times \left[\frac{-2}{e^{(-1)^i k\pi} + e^{(-1)^{i+1} k\pi}} \lim_{r\to 0} \sigma_{yi}\sqrt{2r}\cos(k\log r) + \frac{2}{e^{(-1)^i k\pi} - \mu_i e^{(-1)^{i+1} k\pi}} \lim_{r\to 0} \mu_i \sigma_{xyi}\sqrt{2r}\sin(k\log r) \right] \quad (4)$$

$$\tilde{K}_2 = e_i \frac{\bar{E}\bar{h}(3+\bar{\nu})(1-\nu_i^2)}{E_i h_i (3+\nu_i)(1-\bar{\nu}^2)} \times \left[\frac{-2}{e^{(-1)^i k\pi} + e^{(-1)^{i+1} k\pi}} \lim_{r\to 0} \sigma_{yi}\sqrt{2r}\sin(k\log r) - \frac{2}{e^{(-1)^i k\pi} - \mu_i e^{(-1)^{i+1} k\pi}} \lim_{r\to 0} \mu_i \sigma_{xyi}\sqrt{2r}\cos(k\log r) \right] \quad (5)$$

where $e_1=1$, $e_2=\mu_2/\gamma\mu_1$, and $i=1$ or 2; i.e., whether the stress intensity factors are calculated from material 1 or 2 or any direction, there will be the same limit values. Therefore, the stress intensity facors under this definition may be used to represent the intensity of stress singularity near the crack tip.

Common Interelement Boundary Displacement and Normal Slope (w^*,θ_n^*)

Since the singular element may be adjacent to regular or other singular elements,[6] the assumed interpolation function

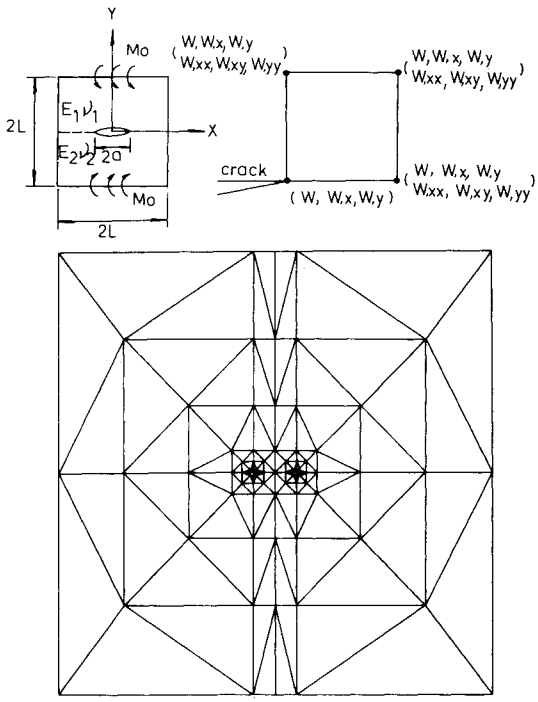

Fig. 1 The bending analysis of bimaterial center-cracked plate ($a/L=0.1$).

$[L]$ in Eq. (2) is divided into two types:

1) The boundary adjacent to a regular element. To satisfy the compatibility requirement, the assumed interpolation function for (w^*,θ_n^*) along the boundary adjacent to a regular element should be of the same type as that of the regular elements. Since Bell's 18 degrees of freedom conforming to the triangular plate bending element[8] are employed in this work, w^* and θ_n^* are assumed to be

$$w^* = a_0 + a_1\xi + a_2\xi^2 + a_3\xi^3 + a_4\xi^4 + a_5\xi^5$$

$$\theta_n^* = b_0 + b_1\xi + b_2\xi^2 + b_3\xi^3$$

where $\xi(-1\le\xi\le 1)$ is the local coordinate along the boundary line and $a_0, a_1,\ldots,a_5$, and $b_0, b_1,\ldots,b_3$ can be computed in terms of the relevant nodal values $\{q\}$, thus determining $[L]$.

2) The boundary adjacent to a singular element. To match the singular and oscillatory characters of stresses near the crack tip, $[r^{3/2}\cos(k\log r), r^{3/2}\sin(k\log r)]$ and $[r^{1/2}\cos(k\log r), r^{1/2}\sin(k\log r)]$ are embedded into the interpolation functions for w^* and θ_n^*, respectively. It is noted

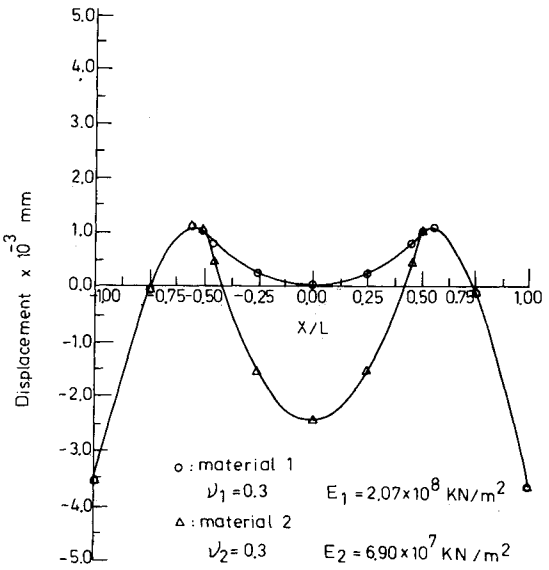

Fig. 2 The transverse deflection along the upper and lower interfaces.

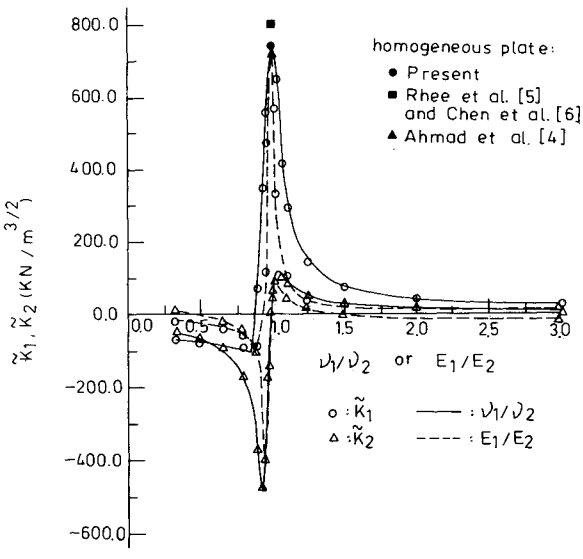

Fig. 3 Variations of $\tilde{K}_1$ and $\tilde{K}_2$ vs different material properties.

that, due to the singular behaviors, the second-order derivatives of the lateral displacement w do not exist at the crack tip. Thus, (w^*,θ_n^*) should be assumed to be

$$w^* = a_0 + a_1 r + a_2 r^2 + a_3 r^{3/2}\cos(k\log r) + a_4 r^{3/2}\sin(k\log r)$$

$$\theta_n^* = b_0 + b_1 r^{1/2}\cos(k\log r) + b_2 r^{1/2}\sin(k\log r)$$

Again, the parameters a_0, $a_1,\ldots,a_4$ and b_0, b_1, b_2 can be determined in terms of the appropriate nodal variables along the boundary.

3) Element equivalent boundary transverse shear and bending moment (V_n,M_{nn}). The regular portion of the bending stress fields can be assumed as that in Ref. 6. For the singular portion, however, it is assumed to be

$$\begin{aligned}
M_{xi} = \frac{\alpha_{23}}{\sqrt{r}}\Bigg\langle &\Bigg\{[-3-5\nu_i+(6+2\nu_i)C_i]\cos\frac{\theta}{2} \\
&+(1-\nu_i)\cos\frac{5\theta}{2}+k(1-\nu_i)\left(\sin\frac{5\theta}{2}-\sin\frac{\theta}{2}\right)\Bigg\}\cos\epsilon \\
&+\Bigg\{[3+5\nu_i+(6+2\nu_i)C_i]\sin\frac{\theta}{2} \\
&-(1-\nu_i)\sin\frac{5\theta}{2}+k(1-\nu_i)\left(\cos\frac{5\theta}{2}-\cos\frac{\theta}{2}\right)\Bigg\}\sin\epsilon\Bigg\rangle \\
+\frac{\alpha_{24}}{\sqrt{r}}\Bigg\langle &\Bigg\{[-3-5\nu_i-(6+2\nu_i)C_i]\sin\frac{\theta}{2} \\
&+(1-\nu_i)\sin\frac{5\theta}{2}-k(1-\nu_i)\left(\cos\frac{5\theta}{2}-\cos\frac{\theta}{2}\right)\Bigg\}\cos\epsilon \\
&+\Bigg\{[-3-5\nu_i+(6+2\nu_i)C_i]\cos\frac{\theta}{2} \\
&+(1-\nu_i)\cos\frac{5\theta}{2}+k(1-\nu_i)\left(\sin\frac{5\theta}{2}-\sin\frac{\theta}{2}\right)\Bigg\}\sin\epsilon\Bigg\rangle
\end{aligned}$$

$$\begin{aligned}
M_{yi} = \frac{\alpha_{23}}{\sqrt{r}}\Bigg\langle &\Bigg\{[-5-3\nu_i-(6+2\nu_i)C_i]\cos\frac{\theta}{2} \\
&-(1-\nu_i)\cos\frac{5\theta}{2}-k(1-\nu_i)\left(\sin\frac{5\theta}{2}-\sin\frac{\theta}{2}\right)\Bigg\}\cos\epsilon \\
&+\Bigg\{[5+3\nu_i-(6+2\nu_i)C_i]\sin\frac{\theta}{2} \\
&+(1-\nu_i)\sin\frac{5\theta}{2}-k(1-\nu_i)\left(\cos\frac{5\theta}{2}-\cos\frac{\theta}{2}\right)\Bigg\}\sin\epsilon\Bigg\rangle \\
+\frac{\alpha_{24}}{\sqrt{r}}\Bigg\langle &\Bigg\{[-5-3\nu_i+(6+2\nu_i)C_i]\sin\frac{\theta}{2} \\
&-(1-\nu_i)\sin\frac{5\theta}{2}+k(1-\nu_i)\left(\cos\frac{5\theta}{2}-\cos\frac{\theta}{2}\right)\Bigg\}\cos\epsilon \\
&+\Bigg\{[-5-3\nu_i-(6+2\nu_i)C_i]\cos\frac{\theta}{2} \\
&-(1-\nu_i)\cos\frac{5\theta}{2}-k(1-\nu_i)\left(\sin\frac{5\theta}{2}-\sin\frac{\theta}{2}\right)\Bigg\}\sin\epsilon\Bigg\rangle
\end{aligned}$$

$$\begin{aligned}
M_{xyi} = \frac{\alpha_{23}}{\sqrt{r}}\Bigg\langle &\Bigg\{[1-\nu_i+(6+2\nu_i)C_i]\sin\frac{\theta}{2} \\
&+(1-\nu_i)\sin\frac{5\theta}{2}-k(1-\nu_i)\left(\cos\frac{5\theta}{2}-\cos\frac{\theta}{2}\right)\Bigg\}\cos\epsilon \\
&+\Bigg\{[1-\nu_i-(6+2\nu_i)C_i]\cos\frac{\theta}{2} \\
&+(1-\nu_i)\cos\frac{5\theta}{2}+k(1-\nu_i)\left(\sin\frac{5\theta}{2}-\sin\frac{\theta}{2}\right)\Bigg\}\sin\epsilon\Bigg\rangle \\
+\frac{\alpha_{24}}{\sqrt{r}}\Bigg\langle &\Bigg\{[-1+\nu_i+(6+2\nu_i)C_i]\cos\frac{\theta}{2} \\
&-(1-\nu_i)\cos\frac{5\theta}{2}-k(1-\nu_i)\left(\sin\frac{5\theta}{2}-\sin\frac{\theta}{2}\right)\Bigg\}\cos\epsilon \\
&+\Bigg\{[1-\nu_i+(6+2\nu_i)C_i]\sin\frac{\theta}{2} \\
&+(1-\nu_i)\sin\frac{5\theta}{2}-k(1-\nu_i)\left(\cos\frac{5\theta}{2}-\cos\frac{\theta}{2}\right)\Bigg\}\sin\epsilon\Bigg\rangle
\end{aligned}$$

where M_{xi}, M_{yi}, and M_{xyi} are the bending stresses of plate i, $C_1 = e^{2k(\pi-\theta)}$, $C_2 = e^{-2k(\pi+\theta)}$, and $\epsilon = k\log r$.

As a result, based on the thin-plate thoery, the assumed interpolation functions $[R]$ in Eq. (3) for (V_n,M_{nn}) can be easily obtained by proper differentiations. It is worthwhile to note that the interpolation functions for (V_n,M_{nn}) have 24 terms, which are compatible[6] with those from w.

Results and Discussion

To demonstrate the validity of this work, some numerical solutions are presented and discussed. The geometry, loading conditions, and finite element mesh are shown in Fig. 1. Eight hybrid singular crack elements are surrounded by 136 Bell-conforming triangular elements.

From Eqs. (4) and (5), it is seen that both σ_y and σ_{xy} are included in the expressions for the proposed stress intensity factors $\tilde{K}_1$ and $\tilde{K}_2$. Therefore, $\tilde{K}_1$ and $\tilde{K}_2$ are different from those defined in homogeneous cases where the symmetric and antisymmetric loads are separately introduced. $\tilde{K}_1$ and $\tilde{K}_2$ are the parameters that account for the combined effects of these two different materials. However, further work needs to be done before adopting these as valid fracture parameters that can accurately predict the behaviors of bimaterial cracked plates.

Figure 2 shows the different transverse deflections along the upper and lower interfaces. The variations of $\tilde{K}_1$ and $\tilde{K}_2$ vs different material properties are displayed in Fig. 3. For comparison purposes, the homogeneous plate solution of Ahmad and Loo,[4] Rhee and Atluri,[5] and Chen and Chen[6] are also shown.

Since the present design and the results of Sih and Rice[7] are derived based on the Kirchhoff assumptions, the transverse shear deformation is ignored and the stress boundary conditions are satisfied only approximately. To provide a more general and sophisticated analysis procedure that also considers the transverse shear deformation, Reissner's theory[9] needs to be employed.

References

[1] Barsoum, R. S., "A Degenerate Solid Element for Linear Fracture Analysis of Plate Bending and General Shells," *International Journal for Numerical Methods in Engineering*, Vol. 10, 1976, pp. 551-564.

[2] Moriya, K., "Hybrid Crack Element for Three Dimensional Solids and Plate Bending," Ph.D. Thesis, Massachusetts Institute of Technology, Cambridge, 1977.

[3] Yagawa, G. and Nishioka, T., "Finite Element Analysis of Stress Intensity Factors for Plane Extension and Plate Bending Problems," *International Journal for Numerical Methods in Engineering*, Vol. 14, 1979, pp. 727-740.

[4] Ahmad, J. and Loo, F. T. C., "Solution of Plate Bending Problems in Fracture Mechanics Using a Specialized Finite Element

Technique," *Engineering Fracture Mechanics*, Vol. 11, 1979, pp. 661-673.

[5]Rhee, H. C. and Atluri, S. N., "Hybrid Stress Finite Element Analysis of Bending of a Plate with a Through Flaw," *International Journal of Numerical Methods in Engineering*, Vol. 18, 1982, pp. 259-271.

[6]Chen, W. H. and Chen, P. Y., "A Hybrid-Displacement Finite Element Modal for the Bending Analysis of Thin Cracked Plates," *International Journal of Fracture*, Vol. 24, 1984, pp. 83-106.

[7]Sih, G. C. and Rice, J. R., "The Bending of the Plates and Dissimilar Materials with Cracks," *Journal of Applied Mechanics*, Vol. 31, 1964, pp. 477-482.

[8]Bell, K., "A Refined Triangular Plate Bending Finite Element," *International Journal for Numerical Methods in Engineering*, Vol. 1, 1969, pp. 101-122.

[9]Reissner, E., "The Effect of Transverse Shear Deformation on the Bending of Elastic Plates," *Journal of Applied Mechanics*, Vol. 12, 1945, pp. A-69—A-77.